Concomitant Microbial Generation of Palladium Nanoparticles and Hydrogen To Immobilize Chromate

DEV CHIDAMBARAM,[†] TOM HENNEBEL,[‡] SAFIYH TAGHAVI,[§] JAN MAST,[||] NICO BOON,[‡] WILLY VERSTRAETE,[‡] DANIEL VAN DER LELIE,[§] AND JEFFREY P. FITTS*,[⊥]

Chemical and Materials Engineering, University of Nevada Reno, Reno, Nevada 89557-0388, Laboratory of Microbial Ecology and Technology (LabMET), Ghent University, Coupure Links 653, B-9000 Ghent, Belgium, Biology Department, Brookhaven National Laboratory, Upton, New York 11973-5000, EM-unit of CODA-CERVA, Groeselenberg 99, B-1180 Brussels, Belgium, and Environmental Sciences Department, Brookhaven National Laboratory, Upton, New York 11973-5000

Received May 10, 2010. Revised manuscript received August 10, 2010. Accepted August 16, 2010.

The catalytic properties of various metal nanoparticles have led to their use in environmental remediation. Our aim is to develop and apply an efficient bioremediation method based on *in situ* biosynthesis of bio-Pd nanoparticles and hydrogen. *C. pasteurianum* BC1 was used to reduce Pd(II) ions to form Pd nanoparticles (bio-Pd) that primarily precipitated on the cell wall and in the cytoplasm. *C. pasteurianum* BC1 cells, loaded with bio-Pd nanoparticle in the presence of glucose, were subsequently used to fermentatively produce hydrogen and to effectively catalyze the removal of soluble Cr(VI) via reductive transformation to insoluble Cr(III) species. Batch and aquifer microcosm experiments using *C. pasteurianum* BC1 cells loaded with bio-Pd showed efficient reductive Cr(VI) removal, while in control experiments with killed or viable but Pd-free bacterial cultures no reductive Cr(VI) removal was observed. Our results suggest a novel process where the *in situ* microbial production of hydrogen is directly coupled to the catalytic bio-Pd mediated reduction of chromate. This process offers significant advantages over the current groundwater treatment technologies that rely on introducing preformed catalytic nanoparticles into groundwater treatment zones and the costly addition of molecular hydrogen to above ground pump and treat systems.

Introduction

The catalytic properties of various metal nanoparticles have led to a widespread interest in their use in environmental remediation (*1*). For instance, numerous studies have explored the use of Fe(0) nanoparticles to remove organic and inorganic contaminants (*2*). Recently, the use of more reactive nanoparticles composed of elements belonging to the platinum group has been proposed. However, these remediation strategies are limited by their ability to deliver catalytic nanoparticles plus hydrogen as a suitable electron donor to large treatment zones.

A new biologically inspired method to produce a nano-palladium catalyst involves the precipitation of palladium on a bacterium, resulting in the formation of bio-Pd: when hydrogen is provided, certain bacterial species can reduce Pd(II) and subsequently induce precipitation of Pd(0) nanoparticles on the cell wall and within the periplasmatic space. Two Gram-negative model organisms have been primarily used in this process: the metal-respiring bacterium *Shewanella oneidensis* (*3*) and the sulfate reducing bacterium *Desulfovibrio desulfuricans* (*4*). The reactivity of Pd and bio-Pd nanoparticles as important catalysts in chemical synthesis (*5*) and toward various halogenated groundwater and soil pollutants, such as chlorinated solvents (*6*) and polychlorobiphenyls (*3, 7, 8*) as well as hexavalent chromium (*8*−*10*), has been reported. However, all these processes consist of two-steps, where Pd nanoparticles are formed in a separate reaction before contaminant treatment, thus making these processes less suitable to treat subsurface contaminants. Another limiting step is the need to apply hydrogen *in situ*, which creates both a technical and financial challenge. Indeed, hydrogen gas represented the largest operational cost in pilot-scale reactors applying bio-Pd since large amounts of hydrogen gas were required to charge the nanocatalyst. For example, 60 L of hydrogen gas was needed to remove 2.5 g of TCE in a plate membrane reactor (*6*). Ideally, one would like to design a process for the *in situ* creation of catalytically active nanoparticles that couples the *in situ* production of H_2, which will be used in the Pd biocatalyzed reduction of contaminants. In this manuscript, we describe the proof of concept for this process and subsequently demonstrate its applicability for the improved remediation of chromium.

Clostridium pasteurianum BC1 is an anaerobic hydrogen-producing member of the *Clostridium* group that was isolated from a metal contaminated coal mining site (*11*) and has been shown to possess biochemical pathways that efficiently reduce various contaminant metals and radionuclides (*12*). *C. pasteurianum* was selected as a model organism to examine the viability of a process that combines bio-Pd formation and the charging of the bio-Pd catalyst with reactive hydrogen species. Hexavalent chromium, which is considered to be one of the most prevalent inorganic pollutants and is proven to be acutely toxic, mutagenic, and carcinogenic (*13*), was chosen as a model contaminant. Its reduced form, Cr(III), is not known to be carcinogenic (*14*) and can readily precipitate as $Cr(OH)_3$ under neutral to slightly basic pH. Therefore, the reduction of Cr(VI) to Cr(III) is a key step in the removal of Cr(VI) from aqueous solution (*15*).

The first objective of this study was to examine the *in situ* formation of Pd nanoparticles by *C. pasteurianum*. Additionally, the concomitant microbial generation of Pd nanoparticles and hydrogen was evaluated as a process to immobilize chromate both in aqueous solution and in aquifer microcosms.

Materials and Methods

Microbial Synthesis of Pd Nanoparticles. *C. pasteurianum* BC1 (ATCC No. 53464) was grown according to Francis and Dodge (*16*) in a medium containing (per liter) glucose, 5.0 g; NH_4C1, 0.5 g; glycerol phosphate, 0.3 g; $MgSO_4 \cdot 7H_2O$, 0.2 g; $CaCl_2 \cdot 2H_2O$, 0.5 g; $FeSO_4 \cdot 7H_2O$, 2.8 mg; peptone, 0.1 g; and

* Corresponding author phone: (631)344-2777; fax: (631)344-2287; e-mail: fitts@bnl.gov.
[†] University of Nevada Reno.
[‡] Ghent University.
[§] Brookhaven National Laboratory.
[||] EM-unit of CODA-CERVA.
[⊥] Brookhaven National Laboratory.

10.1021/es101559r
Published on Web 09/07/2010

yeast extract, 0.1 g. The pH of the medium was adjusted to 6.8 using 1 M NaOH. Reagents were deoxygenated by boiling and purging with nitrogen, prior to being transferred to an anaerobic glovebox where 22.5 mL aliquots of the medium was dispensed into 33 mL serum bottles. All gases used were ultrahigh purity grade. The bottles were sealed with butyl rubber stoppers and aluminum crimps and autoclaved prior to inoculation with *C. pasteurianum*. Cultures were grown in an incubator (125 rpm shaker table, 27 C) until reaching the end of the log phase of growth (optical density measured at 600 nm, OD_{600} = 0.6), which typically required approximately 18 h. Unless otherwise stated, all cultures were then spiked with aqueous Pd(II) (1 g L^{-1} Na_2PdCl_4 stock solution) to achieve an initial Pd(II) concentration of 100 mg L^{-1}. Aqueous Pd(II) in the filtered supernatant of representative cultures was determined spectrophotometrically using its complexation reaction with chromazurol (*17*). Control experiments were conducted where Ar was bubbled through the culture for 2 h prior to aqueous Pd(II) addition to purge the biogenic hydrogen from the system. All liquid culture experiments were performed in triplicate. Culture viability and growth relative to a pure culture, which was grown in parallel, was tested after every experiment by comparing the time required for a 1 mL inoculation from every culture to reach OD_{600} of 0.6 in fresh media.

Analysis of Morphology and Speciation of Bio-Pd in Pure Batch Cultures. The bio-Pd loaded biomass was harvested by centrifugation for 20 min at 5000 rpm. An aliquot of the bio-Pd loaded biomass pellet was air-dried on a silicon substrate and sputter-coated with gold for scanning electron microscopy (SEM) analysis. The bio-Pd morphology and spatial distribution within the biomass were examined using a LEO 1550 SEM equipped with a Schottky Field-Emission Gun.

Ultrathin sections (~50 nm) of subsamples for transmission electron microscopy (TEM) were prepared with the Ultracut microtome (Reichert-Jung A.G., Vienna, Austria) by omitting OsO_4 fixation, uranyl acetate incubation, and Reynold's lead citrate staining from the previously published procedure by Mast and co-workers (*18*). Ultrathin sections were placed on pioloform- and carbon-coated copper grids and were examined using a Technai Spirit TEM (FEI, Eindhoven, Netherlands) at 120 kV.

Subsamples of the biomass pellets were also air-dried on a glass substrate for characterization by X-ray diffraction (Rigaku Ultima III X-ray diffractometer). Subsamples of bio-Pd loaded biomass pellets were also characterized using X-ray absorption fine structure spectroscopy (XAFS) at beamline X11A at the National Synchrotron Light Source (NSLS) using a Si(311) monochromator crystal.

Batch Studies of Cr(VI) Reduction. Hexavalent chromium [Cr(VI)] was added to bio-Pd suspensions using a 520 mg L^{-1} K_2CrO_4 stock solution to achieve an initial Cr(VI) concentration of 26 mg L^{-1}. As controls for Cr(VI) removal Pd free living or autoclaved cell suspensions with an OD_{600} of 0.6 were used. The concentration of soluble Cr(VI) in subsamples removed from the cultures at different time intervals was determined spectrophotometrically using its complexation reaction with diphenylcarbazide in an acidic solution (*19*), which had a working detection limit of 0.5 mg L^{-1}.

Aquifer Microcosms. The pure culture batch experiments were repeated in the presence of quartz sand in order to challenge bio-Pd formation and its catalytic activity within a mineral matrix that mimics the porosity and permeability of a loosely packed sandy aquifer. Sand microcosm experiments were performed using chromatography columns (120 mL volume, 4.45 cm diameter, 33 cm height) (Chromatography Research Supplies 202242, USA) packed with 175 ± 3 g of size-fractionated quartz sand, which was held in place at the inlet and outlet ports by layers of larger pebbles. The influent was pumped into the bottom end of the columns from anaerobic 2 L influent vessels using a peristaltic pump (Watson Marlow, USA). The effluents were collected at the top of the columns in separate 2 L vessels or diverted to syringes for subsample collection at predetermined time intervals. The columns were packed by alternatively adding autoclaved sand and pumping growth medium to achieve close packing and minimize preferential flow paths. Subsequently a 10 mL *C. pasteurianum* BC1 inoculum, which was previously grown until reaching the stationary phase (OD_{600} = 1.15), was injected directly into the column. Initially, the bacteria were allowed to attach to sand grains and form biofilm coatings without flow for 18 h, after which the same growth medium used in the batch studies (see description above) was sent through the column at a flow rate of 12.5 mL h^{-1}. This flow rate was continued for between 6 and 8 h until anaerobic conditions were confirmed by adding 1 mg resazurin L^{-1} to column effluent bottles. As an abiotic control, an equivalent aquifer microcosm was set up with the addition of 0.5 M formaldehyde to the influent medium, which is known to prevent bacterial growth and biofilm formation (*20*).

Once anaerobic conditions were established, the influent solutions of the sand aquifer microcosm and abiotic control were spiked with 50 mg L^{-1} of aqueous Pd(II) and pumped into the columns during 8 h at a flow rate of 12.5 mL h^{-1}. Subsequently, Pd-free medium was pumped through the columns for 12 h to flush any remaining aqueous Pd species. While maintaining anaerobic conditions, approximately 1 cm^3 subsamples of the sand were removed from the bottom and top of the columns (approximately 5 cm below the top surface of each end of the column) for X-ray microprobe analyses (see below) in order to characterize the spatial distribution and chemical speciation of any Pd associated with the sand matrix. In a second stage, the influent growth medium was spiked with 13 mg L^{-1} Cr(VI) and continuously pumped for 8 h at a flow rate of 12.5 mL h^{-1}. The Cr(VI) concentration of the effluent was determined every 2 h and represents an average Cr concentration in the effluent over 2 h of collection. Upon completion of the experiment, the sand was again sampled at the bottom and the top of the columns for X-ray microprobe analyses of Pd and Cr spatial distribution and chemical speciation.

Pd and Cr Speciation Determination. All micro X-ray fluorescence (μXRF) imaging and micro X-ray absorption near-edge structure (μXANES) spectroscopy measurements were performed using the microprobe beamline X27A at the NSLS. Sand subsamples collected from the microcosm experiments were dispersed in a thin, single grain layer on a high purity silica disk and sealed with a polypropylene film. Samples were secured to a x,y,z motorized stage 45 to the incident beam and 13-element HGe Canberra fluorescence detector. The beam spot-size on the sample was maintained at ca. 15 × 10 μm. Initially, two-dimensional μXRF maps (incident energy 24.6 keV, 0.01 mm x,y step size) recorded the spatial distribution of Pd fluorescence within three 1 mm^2 areas of each sample. Pd distribution maps (background subtracted, integrated peak intensity) were used to identify regions of interest to collect Pd and Cr K-edge μXANES point spectra. A Si(311) monochromator crystal was used during all μXRF mapping and μXANES spectra collection (0.5 and 0.1 eV step sizes through the Pd and Cr K-edge regions, respectively). Pd and Cr XANES spectra were calibrated to the first-derivative maximum of a Pd metal foil (24350 eV) and Cr metal foil (5989 eV), respectively. Identical background subtraction and normalization to edge-height processing was performed on all μXANES spectra of a given element following standard methods (*21*).

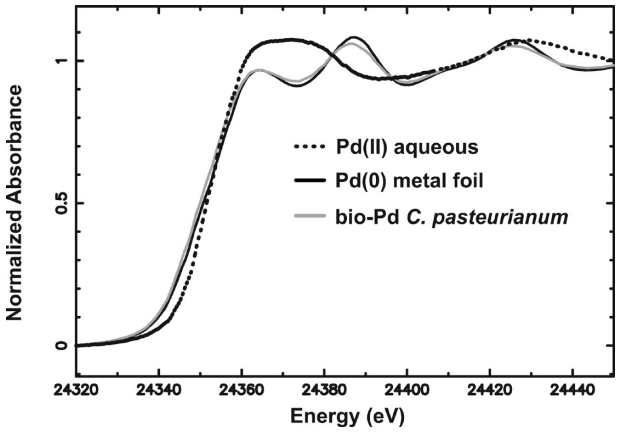

FIGURE 1. XANES spectra of fully hydrated bio-Pd biomass pellet sample, Pd(II) aqueous solution, and Pd(0) metal foil indicating the zerovalent, metallic nature of the biogenic palladium precipitates.

Results and Discussion

Formation of Pd Nanoparticles by C. pasteurianum BC1. *C. pasteurianum* BC1 glycolysis produces fermentation products including hydrogen, acetate, butyrate, and formate that create a highly reducing environment. When a culture of *C. pasteurianum* BC1 (18 h, $OD_{600} = 0.6$) was spiked with aqueous Pd(II) at an initial Pd concentration of 100 mg L^{-1}, the medium turned black within one minute, and the aqueous Pd concentration was below a detection limit of 1 mg L^{-1}. In contrast, an abiotic control starting with 100 mg L^{-1} aqueous Pd(II) in sterile growth media showed neither a color change nor a reduction in Pd(II) ion concentration, and, therefore, compounds in the growth medium do not significantly complex with Pd(II) ions or contribute measurably to Pd(II) reduction. The black color change has previously been reported under comparable conditions with *Shewanella oneidensis* (*3*) and *Desulfovibrio desulfuricans* (*4*) as an indicator of reductive precipitation of metallic Pd nanoparticles. The reduction of greater than 99% Pd(II) by *C. pasteurianum* BC1 within one minute is remarkably faster than the rates reported for *S. oneidensis* and *D. desulfuricans*, where black precipitates first appear after 5−10 min and complete reduction is only observed after approximately 1 h (*3, 4*).

Pd(II) toxicity toward *C. pasteurianum* BC1 was assessed by equilibrating the medium with aqueous Pd(II) at initial concentrations of 25, 50, 100, 200, and 500 mg L^{-1} Pd(II) prior to inoculation. Enumeration by standard plate counts showed that Pd(II) did not significantly inhibit bacterial growth relative to a Pd-free culture at any of the Pd(II) concentrations tested. Moreover, a black suspension formed during the 48 h incubation period in all of the Pd-containing cultures. These observations indicate that Pd(II) did not show significant toxicity toward *C. pasteurianum* BC1 and that bio-Pd nanoparticles also form during the growth phase. In contrast, Pd(II) toxicity was observed with *S. oneidensis*, although cells easily recovered and resumed growth when a suitable electron donor was supplied (*7*).

The XANES and XRD results confirm that aqueous Pd(II) ions were reduced to metallic Pd(0) and precipitated as crystalline nanoparticles in the cultures of *C. pasteurianum* BC1. The XANES spectra shown in Figure 1 compare bio-Pd with an aqueous Pd(II) solution and a Pd(0) metal foil. The coincidence of the edge positions of the bio-Pd and Pd metal foil (26,450 eV) and their shift relative to the edge position of aqueous Pd(II) (26,452 eV) indicate that full reduction of Pd(II) has occurred. The X-ray powder diffractograms (Figure S1) compare a metallic Pd black standard with an air-dried bio-Pd sample. The glass slide mount is responsible for the broad peak in the bio-Pd diffractogram. The coincidence of all Bragg diffraction peaks characteristic of metallic Pd indicates that the bio-Pd nanoparticles are both metallic and crystalline. The broadening of the bio-Pd peaks arises from the nanoscale size of the bio-Pd particles and contrasts with the sharp peaks of the Pd black particles that are larger than 200 nm.

SEM analyses shows that a significant portion of the bio-Pd was deposited on the microbial surface (Figure 2A,B; see Supporting Information (SI) Figure S2 for additional images). Samples of bio-Pd, obtained after addition of 2, 20, 50, and 100 mg L^{-1} aqueous Pd(II) to a cell culture with an OD_{600} of 0.6, were analyzed by TEM. Representative images are shown in Figure 2C,D. TEM images indicate the Pd(0) nanoparticle deposition occurs both on the cell wall and within the cytoplasm of *C. pasteurianum* BC1, as opposed to *S. oneidensis* where nanoparticle deposition was only observed on the cell wall and in the periplasm. In addition, electron-dense precipitates in zones where no bacteria were present appear to be amorphous Pd(0) precipitates and aggregates that either formed on cell debris or resulted from the destruction of cells during TEM sample fixation process. TEM results also indicate that the starting Pd(II) concentration for a given cell density does not systematically impact the size-distribution of Pd nanoparticles. The size-distribution of particles (11.8 ± 4.5 nm mean size; see SI Figure S3 for nanoparticle size distribution histogram) in all samples varied from less than 1 to 15 nm. This result contrasts to earlier findings for *S. oneidensis*, where decreasing the ratio of Pd(II) concentration to cell dry weight produced smaller diameter nanoparticles (*7*).

C. pasteurianum BC1 cultures, which were flushed with Ar to purge the hydrogen produced by *C. pasteurianum* BC1 (biohydrogen) prior to Pd(II) solution addition, required 1 h to achieve the colorimetric change indicative of bio-Pd nanoparticle formation. This result suggests that the biohydrogen produced by *C. pasteurianum* BC1 (see ref *16* for gas production) contributes significantly to the relatively rapid rate of bio-Pd formation. Although purging the excess biohydrogen significantly reduces the rate of bio-Pd formation, *C. pasteurianum* BC1 in the stationary phase still proceeds to complete reductive precipitation of Pd(II). These observations suggest that the formation of bio-Pd can proceed via two primary mechanisms: (i) enzymatic reduction, which is responsible for Pd(II) reduction in the absence of biohydrogen, and (ii) chemical reduction, whereby Pd(II) is reduced by biogenic hydrogen.

Catalyzed Cr(VI) Reduction in Liquid Batch Cultures. The second phase of the research investigated the catalytic properties of the bio-Pd nanoparticles by adding 26 mg L^{-1} chromate to a batch culture approximately 30 min after addition of 100 mg L^{-1} of aqueous Pd(II), and, therefore, after bio-Pd formation is complete. The concentration of free chromate ions was determined using spectrophotometric analysis as a function of time. Figure 3 shows that 45 ± 4% of the Cr(VI) was removed after 10 min. Subsequently, the removal rate decreased and a removal of 73 ± 9% was observed after 72 h, at which point the viability and growth potential indicated that it had undergone comparable growth to a pure culture. Control experiments in which 26 mg L^{-1} Cr(VI) was added to autoclaved or viable but Pd-free bacterial cultures ($OD_{600} = 0.6$) showed no Cr(VI) removal during the first 2 h and 30 ± 3% and 28 ± 3% Cr(VI) removal after 72 h, respectively. The 'viable control' and a pure culture showed equivalent growth to a final $OD_{600} = 1.15$ after 72 h, indicating that Cr(VI) addition did not affect growth. The absence of significant Cr(VI) removal during the first hours in the '*viable control*' indicates that growing *C. pasteurianum* BC1 is not capable of removing Cr(VI) in the absence of bio-Pd. The thirty percent Cr(VI) removal observed after 72 h in both

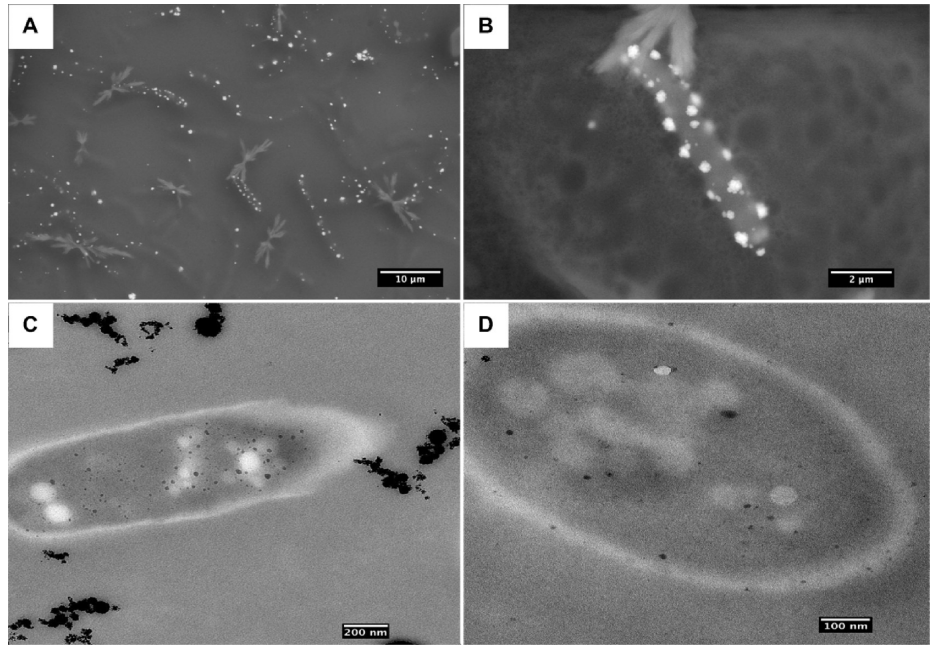

FIGURE 2. Scanning (A, B) and transmission (C, D) electron microscopy of bio-Pd formed by *C. pasteurianum* BC1.

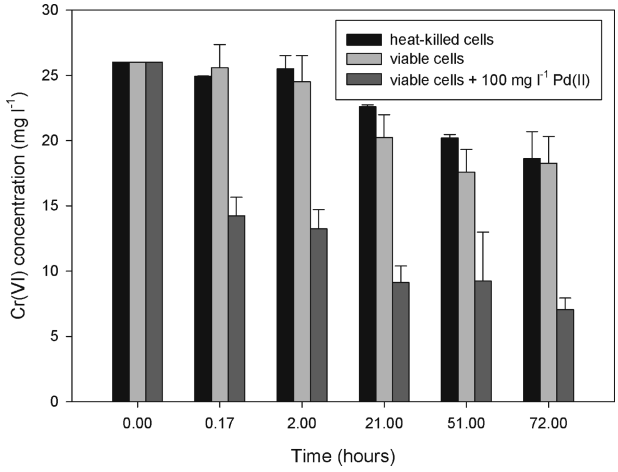

FIGURE 3. The catalytic activity of bio-Pd (100 mg L^{-1} initial aqueous Pd(II)) with respect to Cr(VI) reductive precipitation shown as the removal of Cr(VI) from solution (Cr(VI) initial concentration of 26 mg L^{-1}) as a function of time. Controls consisted of heat-killed and viable *C. pasteurianum* BC1 cells without Pd(II) addition. Mean Cr(VI) concentrations with 2σ standard deviation from triplicate batch cultures are shown.

autoclaved and viable controls is consistent with a simple adsorption mechanism. Moreover, XANES spectra of the Pd-free controls after 72 h did not show measurable Cr(VI) reduction, where the pre-edge peak to step edge-height ratio was equivalent to the 100% Cr(VI) standard aqueous solution. The similar Cr(VI) removal rates observed for the autoclaved and viable Pd-free controls suggest that Cr(VI) removal occurred via adsorption on the biomass and that the combination of bio-Pd and viable *C. pasteurianum* BC1 cells are required to efficiently reduce Cr(VI) to Cr(III).

The reaction product of the Cr(VI) reduction by bio-Pd and biogenic hydrogen was studied using XANES spectroscopy. Figure 4D compares the XANES spectra of the Cr(III)-containing compound CrOOH and an aqueous chromate solution with the XANES spectrum of the wet concentrated biomass pellet of bio-Pd and viable *C. pasteurianum* BC1 8 h after injection with 26 mg L^{-1} of chromate. The absorption edge energy of a XANES spectrum, which is conventionally defined as the first inflection point in the rising edge of the spectrum, is used to compare oxidation states of a given element. The adsorption edge energies of the Cr(III) standard (6000 eV) and the Cr species within the bio-Pd suspension (6002 eV) are both shifted to lower energies relative to the chromate standard solution (6010 eV). The most diagnostic feature, however, is the sharp pre-edge feature in the XANES spectrum of the chromate standard solution, which is a bound state electronic transition that is forbidden in Cr(III) atoms. The absence of this pre-edge feature in the bio-Pd biomass sample spectrum indicates the complete reduction of chromate and the formation of Cr(III)-containing precipitates associated with the bio-Pd biomass.

The Cr(VI) reduction by chemically produced and biogenic Pd nanoparticles using externally added hydrogen gas or formate as electron donor was shown previously (*10, 22*). In the current study a very fast initial removal rate of 7.2 g Cr(VI) g^{-1} Pd h^{-1} (= 140 nmol mg^{-1} Pd h^{-1}) was observed, followed by a much slower reaction rate of 1 mg Cr(VI) g^{-1} Pd h^{-1}. Humphries and Macaskie observed a similar two-stage reduction kinetics using bio-Pd generated by *Desulfovibrio vulgaris* (*23*). These authors, however, reported a significantly higher initial reduction rate (600 nmol mg^{-1} Pd h^{-1}). A comparison of the relative catalytic activity of *C. pasteurianum* bio-Pd and *D. vulgaris* bio-Pd is not instructive given the absence of information about *D. vulgaris* bio-Pd nanoparticle size, which is required to normalize the rates to surface area. In addition, TEM images suggest that the distribution of bio-Pd nanoparticles in the bacterial carrier, and thus, the accessible reactive surface area might differ significantly between the two systems. In the case of *C. pasteurianum* BC1, bio-Pd nanoparticles not only decorate the cell surface but are also located within the cytoplasm, where they are less available for reaction with chromate. In contrast, the bio-Pd nanoparticles formed by *D. vulgaris* are predominantly located on the cell wall, a distribution that will result in a higher active Pd surface area (*24*). The very fast initial removal rate may be inhibited by two important factors: (i) the precipitation of Cr(III)-hydroxide on the active Pd surface may poison the catalyst and (ii) the exhaustion of reactive hydrogen species which had been loaded into the bio-Pd nanoparticles during fermentation. The latter reactive

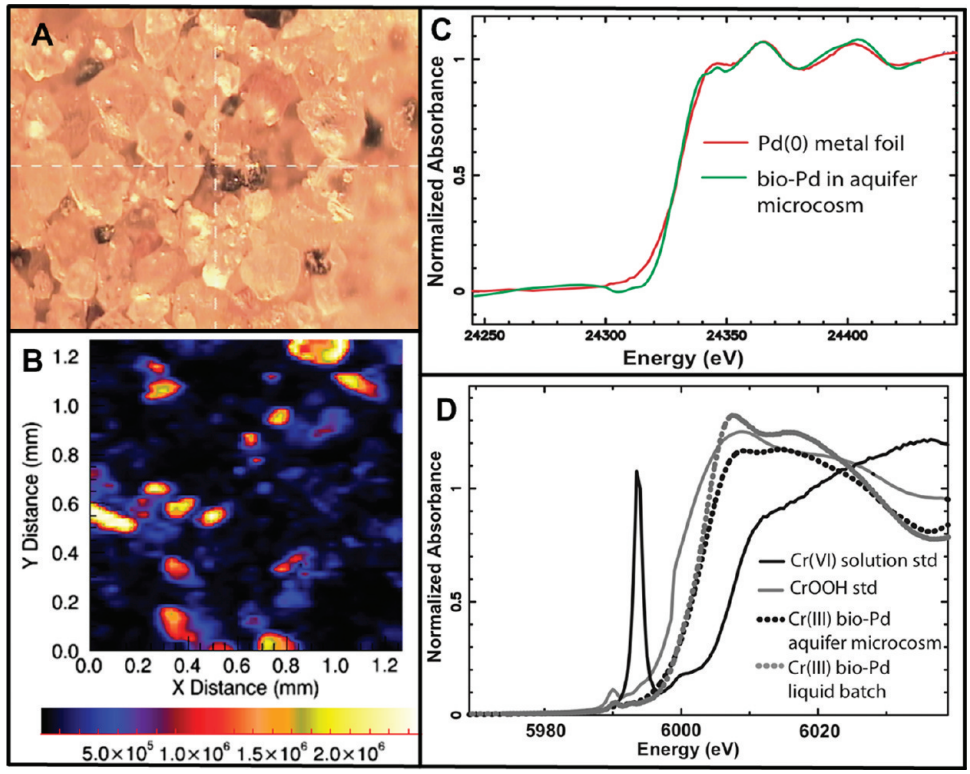

FIGURE 4. Optical image of sand grains containing black precipitates (A), μXRF of Pd distribution (B), and μXANES Pd (C) and Cr (D) K-edge spectra, respectively, showing the presence of Pd(0) and Cr(III) associated with sand grains. (D) Also contains μXANES spectra of Cr after treatment with bio-Pd in liquid batch cultures and standard spectra for Cr(VI) (aqueous chromate) and Cr(III) (CrOOH solid) oxidation states.

biogenic hydrogen species are presumably consumed within the first ten minutes during the fast reaction kinetics.

Two control experiments suggest that the *in situ* biological production of H_2 by *C. pasteurianum* BC1 is essential for both the formation of the bio-Pd catalyst and the subsequent reduction of Cr(VI). First, a culture flushed with Ar prior to Pd(II) addition forms Pd nanocatalysts at a significantly slower rate than a nonpurged culture. Second, an equivalent culture flushed with Ar immediately following bio-Pd formation does not reduce chromate. This second control implicates hydrogen as the electron donor in the reduction of Cr(VI) to Cr(III) at the surface of the bio-Pd catalyst. The introduction of exogenous hydrogen gas following the Ar-flush of this second control failed to restore the catalytic properties of the bio-Pd, and the catalytic reduction of chromate was not observed. These observations all suggest a novel process where the *in situ* microbial production of hydrogen is directly coupled to the catalytic bio-Pd mediated reduction of chromate. Previous studies reported a two-step process, where bio-Pd is produced in a growing culture in the first step, and then the biomass-associated bio-Pd is charged by exogenous hydrogen donors such as formate and hydrogen gas in a second step (*25*). In the case of *C. pasteurianum*, both steps are combined to produce a bio-Pd catalyst charged with active hydrogen species, which are immediately consumable in the reductive precipitation of aqueous Cr(VI).

Chromate Reduction in Aquifer Microcosms. Aquifer microcosm experiments were designed to test the applicability of *in situ* cogeneration of bionanoparticle catalysts and biohydrogen for the remediation of chromate-contaminated groundwater plumes. Three sand-packed columns (viable bio-Pd, viable Pd-free, and sterile abiotic control), which were prepared following the steps described in the Materials and Methods section, were compared for their chromate removal capacity. First, *C. pasteurianum* BC1 microbial communities were established in the two viable columns. The viable bio-Pd and sterile abiotic control columns then received 29 μg of Pd(II) per gram of sand by introducing 50 mg L^{-1} Pd(II) into the influent. The μXRF image shown in Figure 4B shows the distribution of Pd species at the surfaces of sand grains (optical image of sand grains shown in Figure 4A) in a subsample from the viable bio-Pd aquifer microcosm. The spatial distribution of Pd is representative of all sand subsamples collected from both the top and bottom of the viable bio-Pd aquifer microcosm. The Pd "hotspots" in the μXRF images are generally correlated with high Zn fluorescence (data not shown), which we found to be a good proxy for biomass buildup on the sand grains because Zn fluorescence was found to be below background levels on sand grains from the sterile control column. The μXANES spectra shown in Figure 4C indicate metallic Pd is present at the sand grain surface. These results confirm the *in situ* formation of bio-Pd nanoparticles. The addition of Pd(II) to the formaldehyde-treated sterile abiotic control aquifer microcosm did not result in the formation of metallic Pd(0) nanoparticles, confirming the important role of *C. pasteurianum* BC1 in the *in situ* formation of the Pd(0) nanocatalysts.

The viable bio-Pd aquifer microcosm showed efficient removal of Cr(VI), which was measured as the Cr(VI) concentration in 2 h of accumulated effluent, maintaining the Cr(VI) concentration in the effluent at 0.2 mg L^{-1} while flowing an influent groundwater containing 13 mg L^{-1} chromate for 8 h. In contrast, the sterile abiotic control column showed breakthrough of 6 mg L^{-1} after 2 h, complete breakthrough after 4 h, and 83% of the Cr(VI) was recovered in the effluent after 8 h. Figure 4D shows a representative μXANES spectrum of Cr 'hotspots' associated with sand grains from the viable bio-Pd column that confirm the reduction of chromate and the formation of immobilized Cr(III) species. The viable Pd-free control column did lower the Cr(VI) concentration in the effluent to 5.6 mg L^{-1}. However, in this case the Cr(VI) was likely removed by adsorption to the

biofilm-coated sand grains, given that the batch experiments demonstrated that *C. pasteurianum* BC1 does not reduce Cr(VI) in the absence of bio-Pd. Moreover, in contrast to the viable bio-Pd aquifer microcosm, μXRF images did not show Cr 'hotspots', and μXANES spectra did not show any evidence of Cr(III) species.

This is the first study to report on the formation of biogenic Pd nanoparticles by a microbial community growing on sandy aquifer material. In previous studies, bio-Pd was formed by free-living pure cultures under optimal conditions of nutrition, temperature, and redox conditions (*25*). Moreover, the catalytic properties of bio-Pd were until now always tested in aqueous matrices and not in aquifer microcosms. These observations open perspectives for a remediation technology consisting of injecting Pd(II) into an aquifer with the formation of bio-Pd nanoparticles. The fermentation process of *C. pasteuranium* BC1 or other autochthonous bacteria could charge the bio-Pd with reactive hydrogen species and hence make an external supply of hydrogen donors such as hydrogen gas or formate unnecessary. In this way, one can avoid the technical and economical complications related to a homogeneous supply of *ex situ* produced bio-Pd and of a hydrogen donor to a contaminated site. Although the longevity of bio-Pd remains to be demonstrated, these results demonstrate how nanocatalysts might be used to significantly improve Cr(VI) removal rates over traditional *in situ* biostimulation strategies, a concept that can be further exploited for the remediation of other heavy metals, radionuclides, and organic contaminants.

Acknowledgments

This work was funded by the U.S. Department of Energy Office of Science, Office of Biological and Environmental Research, under project KPCH137, and use of the NSLS at BNL was supported by the Office of Basic Energy Sciences under Contract No. DE-AC02-98CH10886. Tom Hennebel was supported by the Fund of Scientific Research-Flanders (FWO, 7741-02). We would like to thank Jim Quinn (Materials Characterization Lab, State University of New York at Stony Brook) for the SEM imaging results.

Supporting Information Available

Figure S1, XRD of bio-Pd biomass; Figure S2, additional SEM images of bio-Pd coated bacteria; and Figure S3, nanoparticle size distribution histograms.This material is available free of charge via the Internet at http://pubs.acs.org.

Literature Cited

(1) Liu, W. T. Nanoparticles and their biological and environmental applications. *J. Biosci. Bioeng.* **2006**, *102*, 1–7.
(2) Zhang, W. X. Nanoscale iron particles for environmental remediation: An overview. *J. Nanopart. Res.* **2003**, *5*, 323–332.
(3) De Windt, W.; Aelterman, P.; Verstraete, W. Bioreductive deposition of palladium (0) nanoparticles on *Shewanella oneidensis* with catalytic activity towards reductive dechlorination of polychlorinated biphenyls. *Environ. Microbiol.* **2005**, *7*, 314–325.
(4) Lloyd, J. R.; Yong, P.; Macaskie, L. E. Enzymatic recovery of elemental palladium by using sulfate-reducing bacteria. *Appl. Environ. Microbiol.* **1998**, *64*, 4607–4609.
(5) Blaser, H. U.; Indolese, A.; Schnyder, A.; Steiner, H.; Studer, M. Supported palladium catalysts for fine chemicals synthesis. *J. Mol. Catal. A: Chem.* **2001**, *173*, 3–18.
(6) Hennebel, T.; Simoen, H.; De Windt, W.; Verloo, M.; Boon, N.; Verstraete, W. Biocatalytic dechlorination of trichloroethylene with bio-Pd in a pilot-scale membrane reactor. *Biotechnol. Bioeng.* **2009**, *102*, 995–1002.
(7) De Windt, W.; Boon, N.; Van den Bulcke, J.; Rubberecht, L.; Prata, F.; Mast, J.; Hennebel, T.; Verstraete, W. Biological control of the size and reactivity of catalytic Pd(0) produced by *Shewanella oneidensis*. *Anton. Leeuw. Int. J. G.* **2006**, *90*, 377–389.
(8) Baxter-Plant, V.; Mikheenko, I. P.; Macaskie, L. E. Sulphate-reducing bacteria, palladium and the reductive dehalogenation of chlorinated aromatic compounds. *Biodegradation* **2003**, *14*, 83–90.
(9) Mabbett, A. N.; Lloyd, J. R.; Macaskie, L. E. Effect of complexing agents on reduction of Cr(VI) by *Desulfovibrio vulgaris* ATCC 29579. *Biotechnol. Bioeng.* **2002**, *79*, 389–397.
(10) Omole, M. A.; K'Owino, I. O.; Sadik, O. A. Palladium nanoparticles for catalytic reduction of Cr(VI) using formic acid. *Appl. Catal., B* **2007**, *76*, 158–167.
(11) Francis, A. J.; Dodge, C. J. Anaerobic microbial dissolution of transition and heavy metal oxides. *Appl. Environ. Microbiol.* **1988**, *54*, 1009–1014.
(12) Francis, A. J.; Dodge, C. J.; Lu, F. L.; Halada, G. P.; Clayton, C. R. Xps and xanes studies of uranium reduction by *Clostridium* sp. *Environ. Sci. Technol.* **1994**, *28*, 636–639.
(13) Valko, M.; Morris, H.; Cronin, M. T. D. Metals, toxicity and oxidative stress. *Curr. Med. Chem.* **2005**, *12*, 1161–1208.
(14) Lippard, S. J.; Berg, J. M. *Principles of bioinorganic chemistry*; University Science Books: Mill Valley, CA, 1994.
(15) Mabbett, A. N.; Lloyd, J. R.; Macaskie, L. E. Reduction of Cr(VI) by "Palladized" - Biomass of *Desulfovibrio desulfuricans* ATCC 29577. *Biotechnol. Bioeng.* **2004**, *87*, 104–109.
(16) Francis, A. J.; Dodge, C. J. Effects of lead-oxide and iron on glucose fermentation by *Clostridium* sp. *Arch. Environ. Contam. Toxicol.* **1987**, *16*, 491–497.
(17) Ishida, R. Spectrophotometric determination of palladium with chromazurol s. *Bull. Chem. Soc. Jpn.* **1969**, *42*, 1011–1016.
(18) Mast, J.; Nanbru, C.; van den Berg, T.; Meulemans, G. Ultrastructural changes of the tracheal epithelium after vaccination of day-old chickens with the La Sota strain of Newcastle disease virus. *Vet. Pathol.* **2005**, *42*, 559–565.
(19) Urone, P. F. Stability of Colorimetric Reagent for Chromium, S-Diphenylcarbazide, in Various Solvents. *Anal. Chem.* **1955**, *27*, 1354–1355.
(20) Zacharia, Z. A.; Zakaria, Z.; Surif, S.; Ahmad, W. A. Biological detoxification of Cr(VI) using wood-husk immobilized *Acinetobacter haemolyticus*. *J. Hazard. Mater.* **2007**, *148*, 164–171.
(21) Ravel, B.; Newville, M. ATHENA, ARTEMIS, HEPHAESTUS: data analysis for X-ray absorption spectroscopy using IFEFFIT. *J. Synchrotron Radiat.* **2005**, *12*, 537–541.
(22) Mabbett, A. N.; Macaskie, L. E. A new bioinorganic process for the remediation of Cr(VI). *J. Chem. Technol. Biotechnol.* **2002**, *77*, 1169–1175.
(23) Humphries, A. C.; Macaskie, L. E. Reduction of Cr(VI) by palladized biomass of *Desulfovibrio vulgaris* NCIMB 8303. *J. Chem. Technol. Biotechnol.* **2005**, *80*, 1378–1382.
(24) Humphries, A. C.; Mikheenko, I. P.; Macaskie, L. E. Chromate reduction by immobilized palladized sulfate-reducing bacteria. *Biotechnol. Bioeng.* **2006**, *94*, 81–90.
(25) Hennebel, T.; De Gusseme, B.; Boon, N.; Verstraete, W. Biogenic metals in advanced water treatment. *Trends Biotechnol.* **2009**, *27*, 90–98.

ES101559R